MiR-539-3p Alleviates Apoptosis and Extracellular Matrix Degradation in Chondrocytes of Childhood-Onset Osteoarthritis by Targeting RUNX2

Tianming JIN[1], Huabin ZHENG[1], Xiaobing FENG[1], Tianhao WU[1], Kun YANG[1], Yan HUANG[2]

[1]Department of Osteoarthrosis Surgery, Luzhou People's Hospital, Luzhou, Sichuan, China, [2]Department of Neonatal, Luzhou People's Hospital, Luzhou, Sichuan, China

Received November 30, 2023
Accepted February 27, 2024

Summary

Recent research has identified that miR-539-3p impedes chondrogenic differentiation, yet its specific role and underlying mechanisms in childhood-onset osteoarthritis (OA) remain unclear. This study found that miR-539-3p levels were considerably lower in cartilage samples derived from childhood-onset OA patients compared to the control group. Enhancing miR-539-3p expression or suppressing RUNX2 expression notably reduced apoptosis, inflammation, and extracellular matrix (ECM) degradation in OA chondrocytes. In contrast, reducing miR-539-3p or increasing RUNX2 had the opposite effects. RUNX2 was confirmed as a direct target of miR-539-3p. Further experiments demonstrated that miR-539-3p targeting RUNX2 effectively lessened apoptosis, inflammation, and ECM degradation in OA chondrocytes, accompanied by changes in key molecular markers like reduced caspase-3 and matrix metallopeptidase 13 (MMP-13) levels, and increased B-cell lymphoma 2 (Bcl-2) and collagen type X alpha 1 chain (COL2A1). This study underscores the pivotal role of miR-539-3p in alleviating inflammation and ECM degradation in childhood-onset OA through targeting RUNX2, offering new insights for potential therapeutic strategies against this disease.

Key words

Childhood-onset OA • Chondrocytes • miR-539-3p • RUNX2 • ECM degradation

Corresponding author

Y. Huang, Department of Neonatal, Luzhou People's Hospital, Room 1705, Building 15, Zhangba Tianfu Garden Community, Jiangyang District, Luzhou City 646000, Sichuan Province, China. E-mail: huang_yanayna22@yeah.net

Introduction

Osteoarthritis (OA) is a prevalent joint disease characterized by significant pain, loss of function, and potential disability [1]. Emerging research suggest a correlation between youth sports injuries and an elevated risk of developing OA at a younger age [2]. The early stages of OA are marked by a trio of critical processes: an initial yet underappreciated proliferation phase of cartilage-resident cells, the well-documented augmented synthesis, and breakdown of extracellular matrix (ECM) components, along with inflammation [3]. Chondrocytes are the sole cell type in cartilage, and their apoptosis, coupled with ECM degradation, play a pivotal role in cartilage destruction during OA [4,5]. Therefore, investigating the mechanisms of chondrocyte damage could provide valuable insights into the pathology of early-onset OA, particularly in the context of childhood.

MicroRNAs (miRNAs), a substantial group of small non-coding RNAs comprising 19-25 nucleotides, are known to bind to the 3′-untranslated regions (3′-UTR) regions of messenger RNAs (mRNAs), thereby inhibiting protein expression [6]. Several miRNAs are involved in key biological processes like inflammatory response, chondrogenesis, and cartilage remodeling, which are vital in the progression of OA [7,8]. Notably, miR-132 has been identified as a crucial regulator in OA, affecting chondrocyte function through the phosphatase and tensin homolog (PTEN)/ phosphatidylinositol 3-kinase (PI3K)/AKT serine/threonine kinase (AKT) signaling pathway [9]. MiR-15a, on the other hand, inhibits nuclear

factor kappa B (NF-κB) phosphorylation, thereby reducing extracellular matrix degradation and chondrocyte senescence, which can mitigate cartilage degeneration in OA [10]. Additionally, miR-182-5p targets fibroblast growth factor 9 (FGF9), enhancing chondrocyte apoptosis, inflammation, and an OA-like phenotype in rat models [11]. MiR-539-3p has garnered attention in cancer research for its context-dependent roles, functioning as a tumor suppressor in certain contexts [12,13], while acting as an oncogene in others [14]. Beyond cancer, its role in other cellular processes has come under scrutiny. Notably, it was identified as differentially expressed in human adipose-derived stem cells (hASCs) through miRNA microarray analysis [15], marking its potential involvement in diverse cellular pathways. A significant finding by Qin *et al.* [16] revealed that miR-539-3p hinders chondrogenic differentiation of hASCs, specifically by targeting the transcription factor SRY-box transcription factor 9 (Sox-9). This finding emphasizes the miRNA's influence in the differentiation pathways of stem cells.

RUNX2 is known for its pivotal role in chondrocyte maturation, predominantly expressed in the critical stages of pre-hypertrophic and hypertrophic chondrocyte development [17]. Its influence extends to the regulation of key markers associated with chondrocyte hypertrophy and maturation, namely collagen type X alpha 1 chain (COL10A1) and matrix metallopeptidase 13 (MMP-13) [18,19]. Notably, alterations in RUNX2 expression, such as global haploinsufficiency and chondrocyte-specific deletion, have demonstrated protective effects against chondrocyte damage following traumatic knee injuries [20]. Intriguingly, preliminary bioinformatics analysis from this study indicates a potential interaction between miR-539-3p and Runt-related transcription factor 2 (RUNX2). Given the established roles of miR-539-3p in modulating chondrogenic differentiation and the central position of RUNX2 in chondrocyte maturation and response to injury, the study posits an interaction between miR-539-3p and RUNX2, specifically through the miRNA's potential targeting of RUNX2's 3′-UTR. This interaction merits further exploration, particularly in the context of childhood-onset OA, where the miR-539-3p/RUNX2 axis could play a crucial regulatory role.

The objective of this study is to elucidate the role of miR-539-3p and its interaction with RUNX2 in the pathogenesis of childhood-onset OA. Specifically, we focus on understanding how miR-539-3p influences RUNX2 and its subsequent impact on the progression of OA in younger patients. Through this investigation, we aim to uncover new perspectives that could potentially contribute to the development of preventive strategies or therapeutic interventions for childhood-onset OA.

Materials and Methods

Collection of clinical samples

This study involved 12 childhood-onset OA patients (7 Males and 5 Females; Mean age=13.5; 4 Grade I and 8 Grade II) and 12 control subjects, including healthy controls (n=8, 4 Males and 4 Females) and knee contusion (n=4, 3 Males and 1 Female), as control subjects (Mean age=15.4; 4 Grade II). These individuals were treated at the Department of Osteoarthrosis Surgery at Luzhou People's Hospital. From each patient, two types of samples were obtained: articular cartilage tissues *via* arthroscopic techniques and blood using standard venipuncture. The cartilage samples were utilized in two different ways: one for histological staining and the other for molecular analyses, including quantitative real-time PCR (polymerase chain reaction) and western blot. The blood samples, after centrifugation, had their serum used for ELISA (enzyme-linked immunosorbent assay) assays. The study received the necessary ethics approval from the Ethics Committee of Luzhou People's Hospital (Approval No. LPC-A7E). Informed consent was duly obtained from all participating patients as well as their legal guardians.

Histological staining

To evaluate cartilage damage, Alcian Blue (AB) staining and Safranin O-Fast Green (SF) staining techniques were employed. The cartilage tissue samples were first fixed in formaldehyde, then decalcified using an ethylene diamine-tetra acetic acid (EDTA) solution, embedded in paraffin, and sectioned. For AB staining, these sections were submerged in Alcian Blue solution for 30 min or Toluidine Blue solution for 3 min, followed by rinsing in water and alcohol before microscopic examination [21]. This procedure resulted in blue-stained cartilage. For SF staining, the sections were initially dyed with Fast Green for 5 min and subsequently with Safranin O for 2 min, coloring the cartilage red. Osteoarthritis Research Society International (OARSI) scores and cartilage thickness were determined by examination of the SF staining sections [22].

Isolation and culture of articular chondrocytes

Initially, the cartilage tissue was finely diced and then placed in a solution of 0.5 mg/ml trypsin (Sigma-Aldrich, St. Louis, MO) for a duration of 10 min at 37 °C. Post trypsinization, the trypsin was discarded, and the tissue was further processed with 2 mg/ml of type II collagenase (Sigma-Aldrich) for a period ranging from 12 to 16 h. Following this, any tissue fragments that hadn't digested were filtered out using a 100 mm mesh. The fluid part or supernatant was then separated through centrifugation, resulting in the isolation of the chondrocytes. These chondrocytes were then cultured in Dulbecco's Modified Eagle Medium (DMEM) supplemented with 15 % fetal bovine serum (Gibco, USA) and 1 % penicillin/streptomycin (HyClone, USA), maintained at 37 °C with 5 % CO_2. For further experimental use, chondrocytes from the 3rd to 5th generations were selected, identifiable by their staining response to toluidine blue.

Toluidine blue staining

In brief, a 1 % primary solution of toluidine blue was prepared by dissolving 1 g toluidine blue powder in 10 ml of 70 % alcohol. Concurrently, a 1 % solution of NaCl was made by dissolving 1 g of NaCl in 100 ml of distilled water. The working solution of 1 % toluidine blue was then created by mixing 1 ml of the primary toluidine blue solution with 9 ml of the 1 % NaCl solution. Following this, the chondrocytes, once they adhered firmly, were digested to form a cell suspension. This suspension was subsequently inoculated into 6-well plates (1×10^5/ml) and cultured until full adherence was achieved, with confluence surpassing 80 %. The chondrocytes were then gently rinsed twice with PBS and fixed with 4 % paraformaldehyde for 1 h at 4 °C. After fixation, the chondrocytes were washed with tap water for 15 min and then with distilled water for 5 min. Finally, the chondrocytes were stained with the 1 % toluidine blue working solution for 2 h. Images of the stained chondrocytes were captured and photographed using an inverted microscope.

Transfection of interfering RNAs

The miR-539-3p mimics (5′-AUCAUACAA-GGACAAUUUCUUU-3′) (100 nM), mimics NC (5′-UUCUCCGAACGUGUCACGU-3′) (100 nM), miR-539-3p inhibitor (5′-AAAGAAAUUGUCCUUGUA-UGAU-3′) (100 nM), inhibitor NC (5'-ACGUGACAC-GUUCGGAGAA-3') (100 nM), pcDNA4.0-RUNX2 (2 μg), pcDNA4.0 (2 μg), si-RUNX2 and si-NC were purchased from GenePharma Co., Ltd (Shanghai, China). The OA chondrocytes, cultured in 6-well plates to 70-80 % confluence, were transfected with these RNA molecules either individually or in combination as dictated by the experimental design. This transfection process utilized Lipofectamine™ 3000 (Invitrogen, Grand Island, NY) reagent. Following a transfection period of 48 h, the human chondrocytes were collected for subsequent analyses.

ELISA assay

To evaluate the pro-inflammatory cytokines in blood serum and OA chondrocyte samples, ELISA assays were conducted. At first, the serum and supernatants from OA chondrocytes were prepared *via* centrifugation (2000× g for 10-15 min at 4 °C) of blood and OA chondrocytes. Subsequently, the expression levels of interleukin-1 beta (IL-1β), interleukin-6 (IL-6), and tumor necrosis factor-alpha (TNF-α) in serum samples, as well as IL-6 and TNF-α in the supernatants from OA chondrocytes were analyzed following the manufacturer's instructions for each respective ELISA kit (R&D Systems, Minneapolis, MN, USA).

Cell viability assay

To assess the viability of chondrocytes, the Cell Counting Kit-8 (CCK-8) kit (Solarbio, Beijing, China) was employed in accordance with the manufacturer's instructions. Initially, chondrocytes were plated at a density of 4×10^3 cells per well in 96-well plates, with each setup done in triplicate. These cells were then cultured at 37 °C in an atmosphere comprising 95 % air. At designated time points of 0, 24, 48, and 72 h, 10 μl of CCK-8 reagent, diluted in fresh complete media, was added to each well. Following an additional 2 h of incubation at 37 °C, the optical density (OD) of each well was measured at a wavelength of 450 nm using a microplate reader.

Cell apoptosis assessment

The degree of apoptosis in chondrocytes was quantified using the Annexin V-FITC/PI apoptosis detection kit (No. A211-01; Vazyme, Nanjing, China), following the protocol provided by the manufacturer. Initially, chondrocytes, amounting to 5×10^4 cells, were seeded into six-well plates in triplicate. These cells were then simultaneously stained with 10 μl of Annexin V-FITC and PI for 10 min in a dark environment. The

stained cells were subsequently analyzed using flow cytometry (BD FACSCalibur, San Jose, CA, USA). The apoptotic rate was calculated as the cumulative percentage of cells located in both the lower and upper right quadrants of the flow cytometry results.

Bioinformatics analysis and luciferase reporter assay

Bioinformatics analysis was carried out using the TargetScan database, revealing the binding sites of miR-539-3p on the 3'UTR of RUNX2. Utilizing pmirGLO vectors (Promega, Madison, WI, USA), sequences of the RUNX2 3' UTR containing either the native miR-539-3p binding sites or mutant sites were cloned to create luciferase reporter vectors. These were named as WT RUNX2 for the wild-type and MUT RUNX2 for the mutant version. In the luciferase reporter assay, chondrocytes were co-transfected with 200 ng of the respective recombinant plasmid and 200 ng of either miR-539-3p mimics or mimic NC, using Lipofectamine™ 3000 (Invitrogen). After 48 h of transfection, the relative luciferase activity was measured using the Dual-Luciferase system (Promega).

Quantitative real-time PCR

For the quantification of miR-539-3p, the mirVana miRNA isolation kit, TaqMan miRNA reverse transcription kit, and TaqMan miRNA assay kit, all from Thermo Fisher Scientific, USA, were employed. For the quantification of RUNX2, total RNA was extracted from confluent cells using TRIzol reagent (Life Technologies and cDNA was synthesized from 2 μg of the isolated total RNA with the High-Capacity cDNA Reverse Transcription Kit (Applied Biosystems™, Thermo Fisher Scientific, USA). PCR amplifications were conducted using the 7500 real-time PCR system (Applied Biosystems) under specific conditions: an initial 10 min at 95 °C, followed by 40 cycles consisting of 20 s at 95 °C, 30 s at 55 °C, and 30 s at 72 °C. The primer sequences for these amplifications are listed in Table 1. The relative expression levels of each target gene were calculated using the $2^{-\Delta\Delta Ct}$ method with GAPDH as the internal control.

Table 1. Primers for quantitative real-time PCR.

Target Gene	**Forward (5′ – 3′)**	**Reverse (5′ – 3′)**
miR-539-3p	GGAGAAATTATCCTTGGTG	GAACATGTCTGCGTATCTC
RUNX2	CAGTGACACCATGTCAGCAAA	GTCGGCGATGATCTCCACCA
U6	GCATGACGTCTGCTTTGGA	CCACAATCATTCTGCCATCA
GAPDH	TGGTGAAGGTCGGTGTGAAC	TTCCCATTCTCGGCCTTGAC

Western blot analysis

Total proteins were extracted using radioimmunoprecipitation assay (RIPA) lysis buffer and their concentrations determined with a BCA kit (both from Beyotime). For each sample, 30 μg of protein was separated by 10 % SDS-PAGE and then the protein bands were transferred onto polyvinylidene difluoride (PVDF) membranes (Millipore, Billerica, MA, USA). These membranes were blocked with 5 % non-fat milk for 2 h at room temperature. Following this, they were incubated overnight at 4 °C with primary antibodies: anti-RUNX2 (ab76956), anti-caspase-3 (ab184787), anti-Bcl-2 (ab194583), anti-COL2A1 (ab185430), anti-MMP-13 (ab39012), and anti-GAPDH (ab181602), all sourced from Abcam (Cambridge, MA, USA). Subsequently, the membranes were incubated with a horseradish peroxidase-conjugated secondary antibody (ab6721, Abcam) for 2 h at room temperature. The immune-stained protein bands were then detected using enhanced chemiluminescence reagent (Thermo Scientific, Rockford, IL, USA), with GAPDH serving as the loading control.

Statistical analysis

Statistical analysis of the data was conducted using GraphPad Prism software version 8.0. To compare two groups, an unpaired, two-tailed Student's *t*-test was utilized. For comparisons that involved three or more experimental groups, one-way analyses of variance (ANOVA) were performed, followed by Tukey's multiple comparison tests. All data are presented as the mean ± standard deviation (SD). A $p<0.05$ was considered to indicate statistical significance.

Ethics approval and consent to participate

This study was carried out in compliance with the ARRIVE guidelines and all methods were carried out in

accordance with relevant guidelines and regulations. The study received the necessary ethics approval from the Ethics Committee of Luzhou People's Hospital (Approval No. LPC-A7E). Informed consent was duly obtained from all participating patients as well as their legal guardians.

Results

MiR-539-3p expression was downregulated in childhood-onset OA-affected cartilage tissues

Figure 1A illustrated that the cartilage layers in the childhood-onset OA group exhibited a pronounced decrease in AB staining and cell density, in comparison to the control group. Further analysis using SF staining, as shown in Figure 1B, revealed a reduced number of chondrocytes and lower proteoglycan content in the childhood-onset OA group, along with a thinner cartilage layer than in the control group. The OARSI scores, a measure of cartilage injury, were significantly higher in the childhood-onset OA group, as displayed in Figure 1C, which also showed a decrease in cartilage thickness compared to the control group. Additionally, ELISA analyses, detailed in Figure 1D, demonstrated that the levels of pro-inflammatory cytokines (IL-1β, IL-6, and TNF-α) in the blood samples of the childhood-onset OA group were substantially higher than those in the control group. Furthermore, quantitative real-time PCR, as seen in Figure 1E, indicated that the expression levels of miR-539-3p were significantly downregulated in the articular cartilage tissues from the childhood-onset OA group compared to those from the control group.

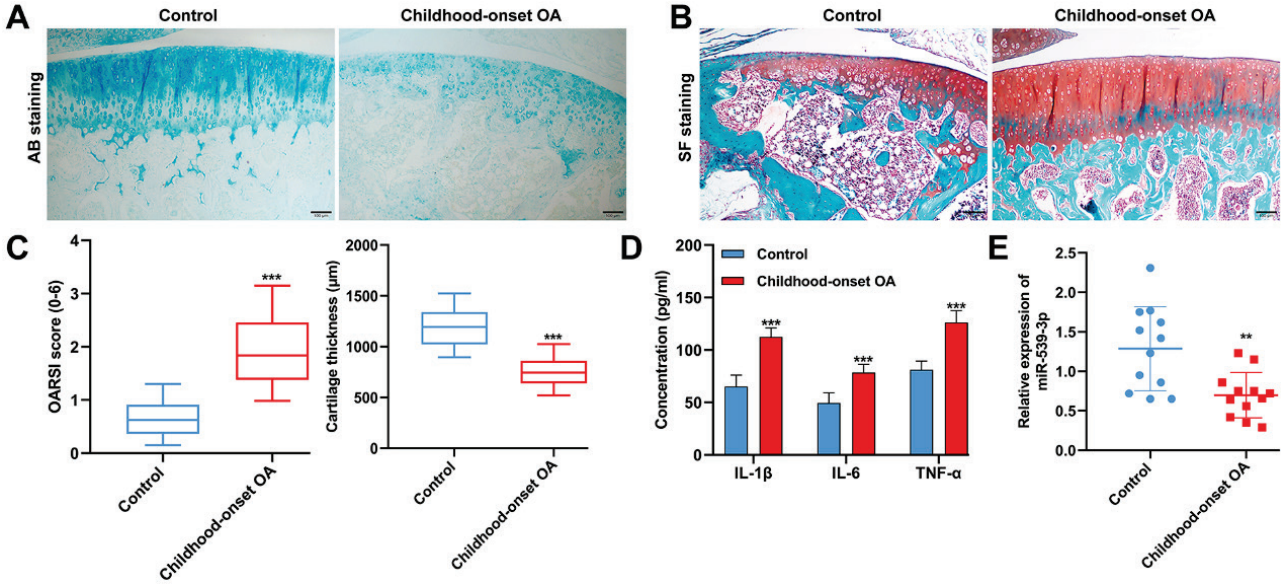

Fig. 1. MiR-539-3p expression was downregulated in childhood-onset OA-affected cartilage tissues. (**A-B**) Morphological changes in cartilage tissue samples derived from childhood-onset OA and control tissues were evaluated by AB staining and SF staining. (**C**) OARSI scores and cartilage thickness were determined by examination of the SF staining sections. (**D**) The levels of IL-1β, IL-6, and TNF-α in blood samples from childhood-onset OA and control patients were analyzed by ELISA assay. (**E**) Quantitative real time PCR was used to detect the levels of miR-539-3p expression in childhood-onset OA and control cartilage tissues. ** p<0.01, *** p<0.001, compared with control. N=12. AB, Alcian Blue staining; SF, Safranin O-Fast Green; OARSI, Osteoarthritis Research Society International.

RUNX2 was a target gene of miR-539-3p

Subsequently, the potential interaction site of miR-539-3p on RUNX2's 3′-UTR was identified using TargetScan, as shown in Figure 2A. To confirm this interaction, chondrocytes were transfected with either WT or MUT RUNX2 luciferase reporter vectors. The findings, presented in Figure 2B, revealed that cells with miR-539-3p overexpression exhibited a significant reduction in luciferase activity when transfected with the WT RUNX2 vectors, but this effect was not observed in the mutant RUNX2 group. Additionally, as Figure 2C indicated, RUNX2 mRNA levels decreased following the overexpression of miR-539-3p and increased when miR-539-3p was silenced in chondrocytes. These results suggest a mechanism where miR-539-3p downregulated RUNX2 by directly targeting its 3'-UTR.

MiR-539-3p attenuated childhood-onset OA chondrocyte injury in vitro

In exploring the biological role of miR-539-3p *in vitro*, chondrocytes from childhood-onset OA cartilage tissues were initially isolated. Figure 3A depicted these

chondrocytes cultured as monolayers, expanding in irregular circular or polygonal shapes. Toluidine blue staining revealed blue-violet cell membranes and cytoplasm, indicating chondrocyte-derived aggrecan. Manipulation of miR-539-3p levels in these chondrocytes involved transfection with miR-539-3p mimics to upregulate and miR-539-3p inhibitor for downregulation, verified by quantitative real-time PCR (Fig. 3B). CCK-8 assay results (Fig. 3C) showed enhanced viability of OA chondrocytes with miR-539-3p overexpression, while miR-539-3p knockdown reduced viability compared to controls. ELISA results (Fig. 3D) demonstrated that miR-539-3p overexpression led to decreased IL-6 and TNF-α levels, whereas its silencing increased these cytokine concentrations. Flow cytometry data (Fig. 3E) indicated that miR-539-3p overexpression reduced apoptosis, but its knockdown significantly increased apoptotic rates. Moreover, overexpressing miR-539-3p increased Bcl-2 and COL2A1 protein expression, but decreased RUNX2, caspase-3, and MMP-13 levels, with the inverse observed following miR-539-3p knockdown (Fig. 3F). Overall, these findings suggest miR-539-3p could enhance cell viability while suppress inflammation, apoptosis, and ECM degradation in OA chondrocytes.

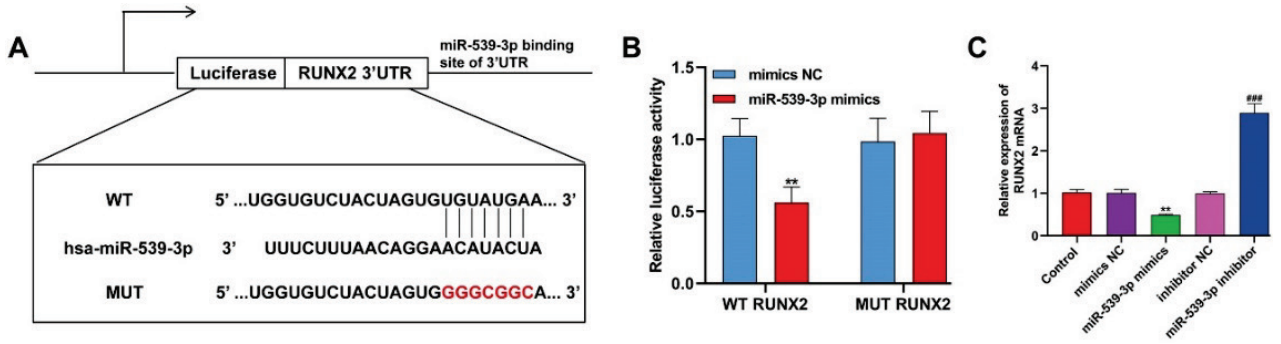

Fig. 2. RUNX2 was a target gene of miR-539-3p. (**A**) Alignment of miR-539-3p and the 3′-UTR of RUNX2, a potential miR-539-3p target. (**B**) A luciferase reporter carrying the 3′-UTR of wild-type (WT) or mutant (MUT) RUNX2 was introduced into chondrocytes along with NC mimic or miR-539-3p mimics. (**C**) The expression levels of RUNX2 mRNA in chondrocytes were determined by quantitative real time PCR. All data were presented as the mean ± SD of three independent experiments. ** p<0.01, compared with mimics NC; ### p<0.001, compared with inhibitor NC.

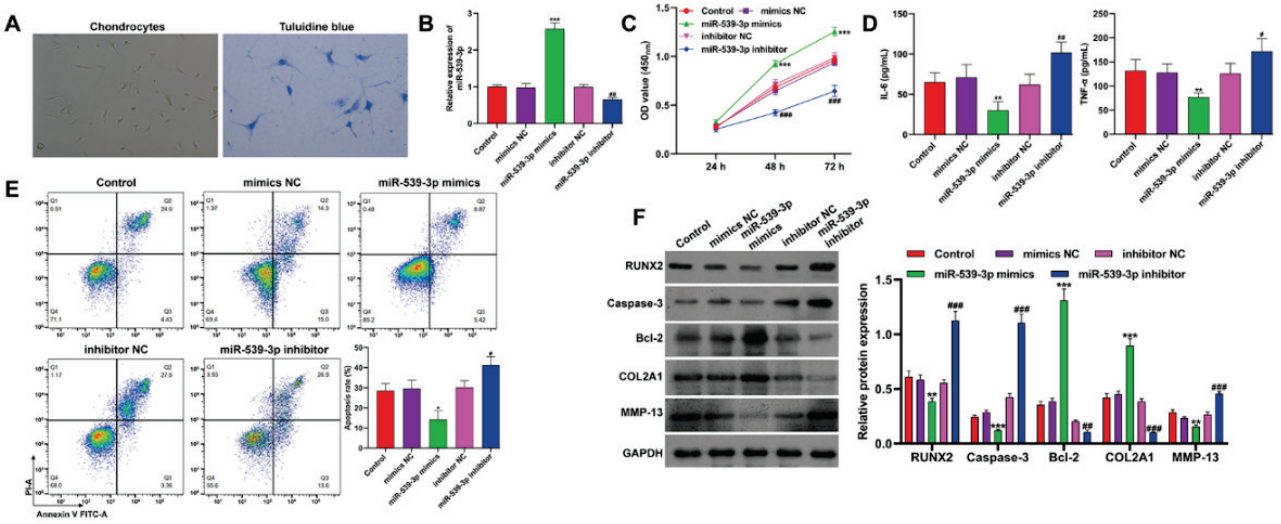

Fig. 3. MiR-539-3p attenuated childhood-onset OA chondrocyte injury *in vitro*. (**A**) The morphology of chondrocytes and results of toluidine blue staining (blue, ×200). Childhood-onset OA chondrocytes were transfected with miR-539-3p mimics, NC mimics, miR-539-3p inhibitor or inhibitor NC for 48 h. (**B**) The expression of miR-539-3p was detected by quantitative real time PCR in transfected chondrocytes. (**C**) Cell viability was analyzed in transfected chondrocytes by CCK-8 assay. (**D**) The concentration of IL-6 and TNF-α in the supernatants of transfected chondrocytes was determined by ELISA assay. (**E**) Cell apoptosis was detected in transfected chondrocytes by flow cytometry. (**F**) The protein levels of RUNX2, caspase-3, Bcl-2, COL2A1 and MMP-13 were detected in transfected chondrocytes by western blot analysis. All data were presented as the mean ± SD of three independent experiments. * p<0.05, ** p<0.01, *** p<0.001, compared with mimics NC; # p<0.05, ## p<0.01, ### p<0.001, compared with inhibitor NC.

RUNX2 deteriorated childhood-onset OA chondrocyte injury in vitro

In the context of RUNX2 being a target of miR-539-3p in chondrocytes, an *in vitro* study was conducted to explore the functional role of RUNX2. The CCK-8 assay findings, as presented in Figure 4A, revealed that the overexpression of RUNX2 significantly reduced the viability of OA chondrocytes, whereas viability was enhanced following RUNX2 knockdown. When RUNX2 was overexpressed, there was an increase in pro-inflammatory cytokines, including IL-6 and TNF-α, in the OA chondrocytes, as shown in Figure 4B-C. Conversely, the reduction of RUNX2 levels led to a decrease in these cytokines. Flow cytometry analysis, depicted in Figure 4D, further demonstrated that RUNX2 over-expression promoted cell apoptosis in OA chondrocytes, while its knockdown had a suppressive effect on apoptosis. On a molecular level, transfection with pcDNA4.0-RUNX2 resulted in upregulated expression of RUNX2, caspase-3, and MMP-13, and a downregulation of Bcl-2 and COL2A1. In contrast, cells transfected with si-RUNX2 exhibited the reverse effects, as shown in Figure 4E.

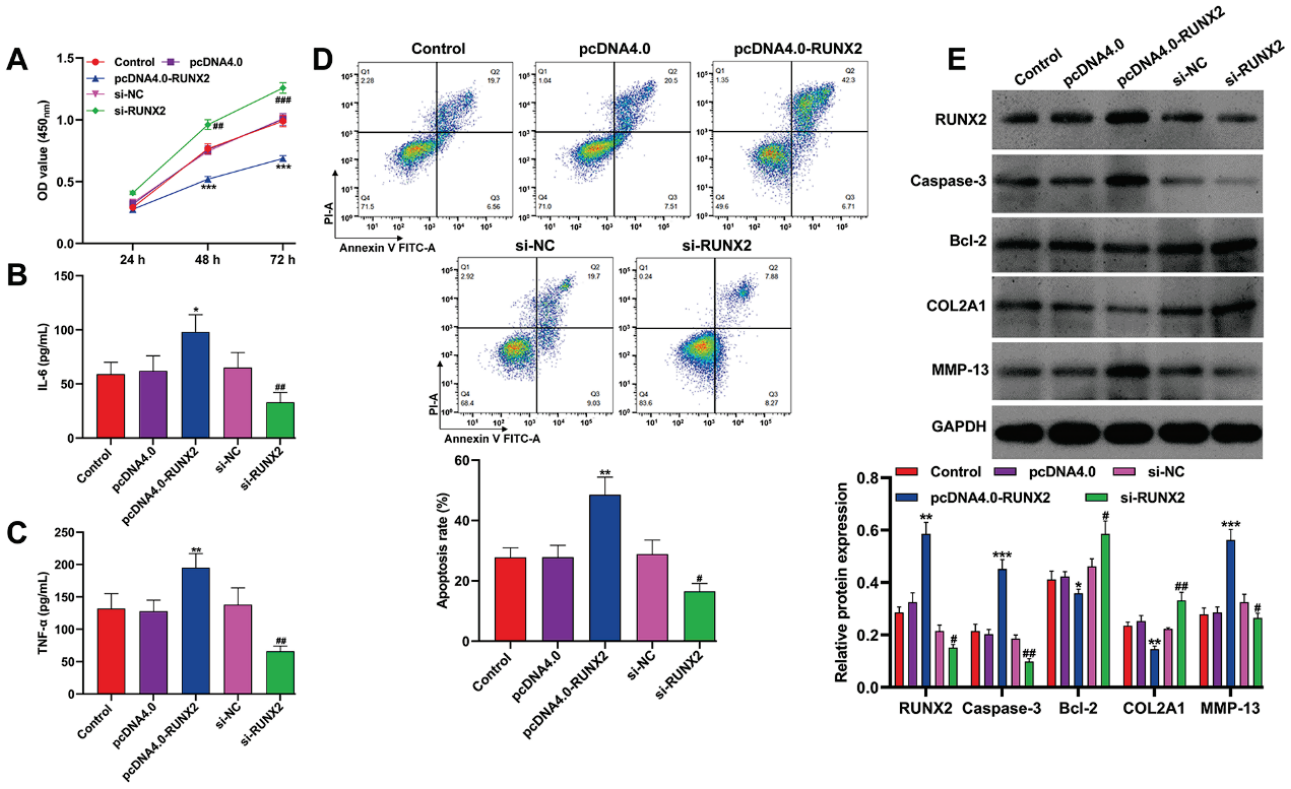

Fig. 4. RUNX2 deteriorated childhood-onset OA chondrocyte injury *in vitro*. Childhood-onset OA chondrocytes were transfected with pcDNA4.0-RUNX2, pcDNA4.0, si-RUNX2, or si-NC for 48 h. (**A**) Cell viability was analyzed in transfected chondrocytes by CCK-8 assay. (**B-C**) The concentration of IL-6 and TNF-α in the supernatants of transfected chondrocytes was determined by ELISA assay. (**D**) Cell apoptosis was detected in transfected chondrocytes by flow cytometry. (**E**) The protein levels of RUNX2, caspase-3, Bcl-2, COL2A1 and MMP-13 were detected in transfected chondrocytes by western blot analysis. All data were presented as the mean ± SD of three independent experiments. * p<0.05, ** p<0.01, *** p<0.001, compared with pcDNA4.0; # p<0.05, ## p<0.01, ### p<0.001, compared with si-NC.

MiR-539-3p inhibited childhood-onset OA chondrocyte injury in vitro through downregulating RUNX2

To investigate whether RUNX2 was a downstream regulator in miR-539-3p-mediated modulation of childhood-onset OA chondrocyte injury, rescue experiments were conducted. These involved co-transfecting chondrocytes with miR-539-3p mimics and pcDNA4.0-RUNX2, or miR-539-3p inhibitor and si-RUNX2. Subsequent functional assays, including the CCK-8 assay (Fig. 5A), ELISA (Fig. 5B-C), and flow cytometry (Fig. 5D), revealed that overexpression of RUNX2 countered the beneficial effects of miR-539-3p mimics on cell viability and their inhibitory impact on pro-inflammatory cytokines (IL-6 and TNF-α) and apoptosis. Similarly, the miR-539-3p inhibitor-induced reduction in cell viability, along with increased levels of

IL-6, TNF-α, and apoptosis, were reversed following RUNX2 knockdown. Additionally, RUNX2 overexpression in chondrocytes transfected with miR-539-3p mimics resulted in increased levels of RUNX2, caspase-3, and MMP-13, and decreased expression of Bcl-2 and COL2A1. Conversely, si-RUNX2 transfection led to the opposite effects in chondrocytes treated with the miR-539-3p inhibitor (Fig. 5E). These findings underscore the role of RUNX2 as a critical factor in the miR-539-3p regulatory pathway, affecting cell viability, inflammation, apoptosis, and ECM degradation in childhood-onset OA chondrocytes.

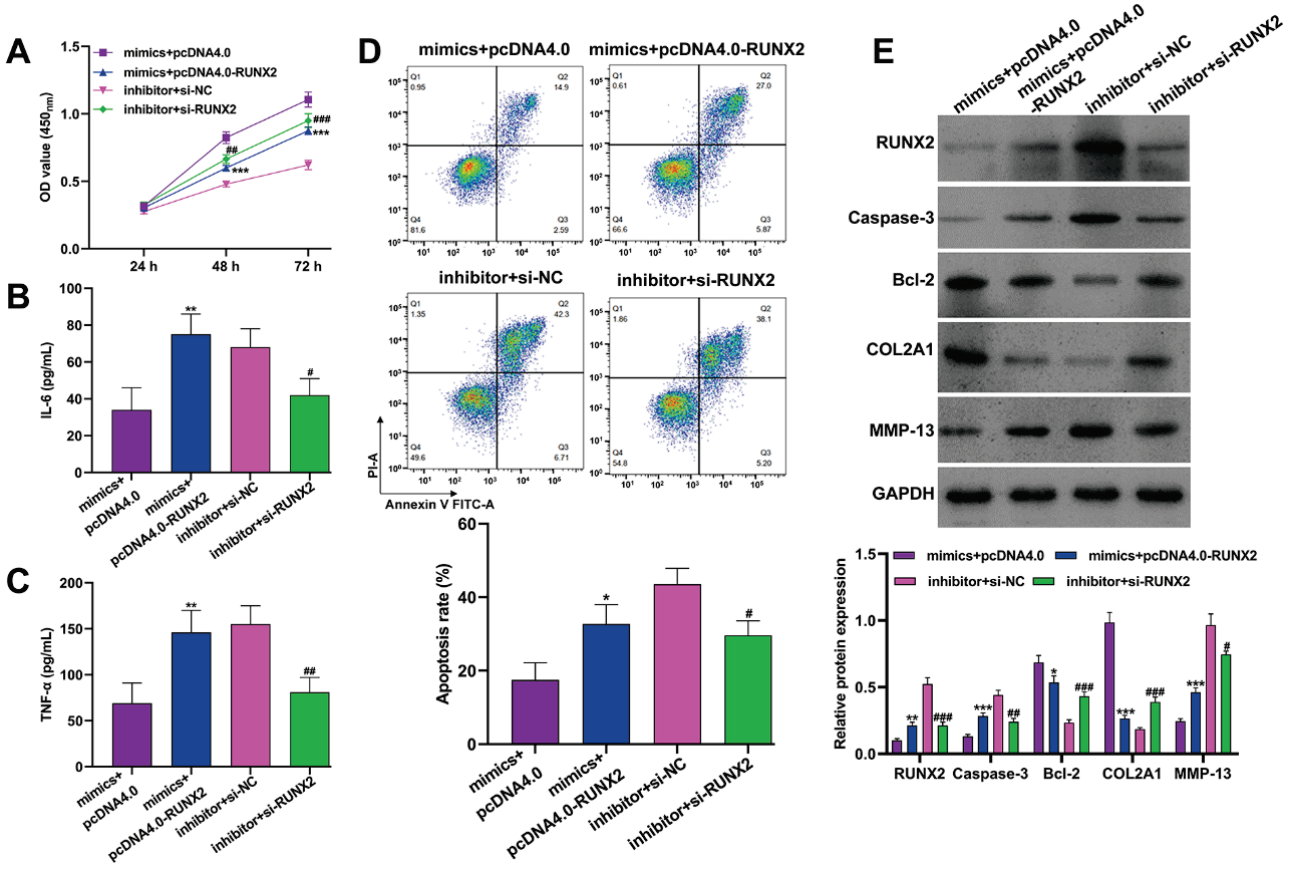

Fig. 5. MiR-539-3p inhibited childhood-onset OA chondrocyte injury *in vitro* through downregulating RUNX2. Childhood-onset OA chondrocytes were co-transfected with miR-539-3p mimics and pcDNA4.0-RUNX2, or miR-539-3p inhibitor and si-RUNX2 for 48 h. (**A**) Cell viability was analyzed in transfected chondrocytes by CCK-8 assay. (**B-C**) The concentration of IL-6 and TNF-α in the supernatants of transfected chondrocytes was determined by ELISA assay. (**D**) Cell apoptosis was detected in transfected chondrocytes by flow cytometry. (**E**) The protein levels of RUNX2, caspase-3, Bcl-2, COL2A1 and MMP-13 were detected in transfected chondrocytes by western blot analysis. All data were presented as the mean ± SD of three independent experiments. * $p<0.05$, ** $p<0.01$, *** $p<0.001$, compared with mimics + pcDNA4.0; # $p<0.05$, ## $p<0.01$, ### $p<0.001$, compared with inhibitor + si-NC.

Discussion

The development of OA in the context of pediatric sports activities has been linked to the degeneration of articular cartilage, primarily due to apoptosis, inflammation, and the degradation of the ECM in chondrocytes [2,23]. MiRNAs, as key gene regulators, play a significant role in modulating these processes, thereby influencing OA progression [24]. Our study found that miR-539-3p exhibited lower expression levels in cartilage tissues from childhood-onset OA patients, suggesting a correlation between miR-539-3p expression and OA-induced cartilage injury. This finding aligns with previous research showing a significant reduction in miR-539 expression in both blood and joint fluid of patients with rheumatoid arthritis (RA) [25]. The differentiation of stem cells into osteogenic and chondrogenic lineages is increasingly recognized for its therapeutic potential in OA, particularly for pain alleviation and enhancement of joint functionality [26]. Supporting this, Yang *et al.* [15] reported a notable alteration in miR-539-3p expression in human adipose-derived stem cells (hADSCs), specifically a minimum two-fold increase, upon chondrogenic differentiation induction.

These observations lead us to propose miR-539-3p as a potential biomarker for the early identification and progression tracking of childhood-onset OA.

Previous research has established the significance of miR-539 in modulating inflammation and cell apoptosis. Hu *et al.* [27] demonstrated that elevated levels of miR-539-5p markedly reduced inflammatory responses, enhanced cell viability and proliferation, and diminished apoptosis in lipopolysaccharide (LPS)-stimulated H9c2 cells. Furthermore, miR-539-5p was found to mitigate sepsis-induced acute lung injury (ALI) by targeting and suppressing rho-associated, coiled-coil containing protein kinase 1 (ROCK1) [28]. Our findings echo these results, indicating that miR-539-3p lowers pro-inflammatory cytokines (IL-6 and TNF-α) and downregulates pro-apoptotic caspase-3, while simultaneously increasing the expression of anti-apoptotic Bcl-2 in chondrocytes affected by childhood-onset OA. This underscores miR-539-3p's inhibitory impact on chondrocyte apoptosis and inflammation. Collagen II (COL-2), a principal component of cartilage ECM [29], is predominantly degraded by MMP-13, a critical enzyme directly linked to OA [30]. MiRNAs are known to play a vital role in regulating ECM degradation. For instance, miRNA-27b-3p, which targets the 3′UTR of MMP-13 mRNA, has been implicated in OA progression [31]. Another miRNA, miR-766-3p, has been reported to significantly reduce apoptosis and enhance autophagy and ECM synthesis in chondrocytes [32]. Considering the established association between the procollagen type II gene (COL2A1) and childhood-onset OA [33], we concluded that miR-539-3p may exert a protective effect against inflammation, apoptosis, and ECM degradation in chondrocytes within the context of childhood-onset OA. Contrary to our findings, Qin *et al.* [16] demonstrated that miR-539-3p inhibits key chondrogenic factors in human adipose stem cells. This discrepancy may arise from differences in cell types (adipose stem cells vs. chondrocytes), stages of cell development, or disease context (chondrogenic differentiation vs. OA). Moreover, miR-539-3p's varying interactions within distinct cellular pathways and methodological variances across studies could contribute to the contrasting results, underlining the molecule's complex role and the necessity for detailed investigation to decipher its multifaceted biological impacts. MiRNAs regulate gene expression by targeting specific genes, inhibiting mRNA and protein synthesis, thereby modulating gene function [34]. RUNX2, a transcription factor belonging to the RUNX family, plays a crucial role in the differentiation of pre-hypertrophic chondrocytes into hypertrophic chondrocytes [35,36]. Overexpression of RUNX2 in chondrocytes leads to accelerated chondrocyte maturation across the entire cartilage structure, including permanent cartilage, which adversely affects joint formation [37]. Additionally, RUNX2 is known to stimulate MMP-1 expression, disrupting the matrix of articular cartilage [19]. Various miRNAs have been identified as targeting the RUNX2 gene, thus influencing OA progression as follows: MiR-204-5p has been shown to reduce chondrocyte proliferation and alleviate OA-like phenotypes in rats with surgically induced OA by targeting RUNX2 [38]. Exosomes from miR-338-3p-modified adipose stem cells (ASCs) were found effective in repairing IL-1β-induced chondrocyte alterations by inhibiting RUNX2 expression [39]. Our recent findings indicate that RUNX2 can be directly targeted by miR-539-3p. However, whether the interaction between miR-539-3p and RUNX2 regulates the process of childhood-onset OA remains to be fully explored. To investigate this, we analyzed the expression of pro-inflammation cytokines, apoptosis and ECM degradation makers in chondrocytes following modulation of the miR-539-3p/RUNX2 axis. The results suggest that miR-539-3p may influence chondrocyte inflammation, apoptosis, and ECM degradation by downregulating RUNX2 expression. The specificity of miR-539-3p's effects in our results may indeed show some similarities with those observed for miR-204-5p [38], which could suggest overlapping functional roles or shared pathways in the biological context we studied. MiR-539-3p and miR-204-5p, although possibly sharing some overlapping functions, are distinct entities with their unique sequences. This uniqueness can lead to differences in their regulation, expression patterns, and ultimately, their biological impact.

In summary, our study demonstrates that miR-539-3p plays a significant role in mitigating chondrocyte apoptosis, inflammation, and ECM degradation *in vitro* through targeting the RUNX2 gene. These insights contribute to a deeper understanding of the function of miR-539-3p in the context of childhood-onset OA. Furthermore, our findings suggest the potential of miR-539-3p as a target for therapeutic interventions aimed at preventing or mitigating the progression of childhood-onset OA.

Conflict of Interest

There is no conflict of interest.

References

1. Ondresik M, Azevedo Maia FR, da Silva Morais A, Gertrudes AC, Dias Bacelar AH, Correia C, Goncalves C, ET AL. Management of knee osteoarthritis. Current status and future trends. Biotechnol Bioeng 2017;114:717-739. https://doi.org/10.1002/bit.26182
2. Caine DJ, Golightly YM. Osteoarthritis as an outcome of paediatric sport: an epidemiological perspective. Br J Sports Med 2011;45:298-303. https://doi.org/10.1136/bjsm.2010.081984
3. Boehme KA, Rolauffs B. Onset and Progression of Human Osteoarthritis-Can Growth Factors, Inflammatory Cytokines, or Differential miRNA Expression Concomitantly Induce Proliferation, ECM Degradation, and Inflammation in Articular Cartilage? Int J Mol Sci 2018;19:2282. https://doi.org/10.3390/ijms19082282
4. Zamli Z, Adams MA, Tarlton JF, Sharif M. Increased chondrocyte apoptosis is associated with progression of osteoarthritis in spontaneous Guinea pig models of the disease. Int J Mol Sci 2013;14:17729-17743. https://doi.org/10.3390/ijms140917729
5. Charlier E, Deroyer C, Ciregia F, Malaise O, Neuville S, Plener Z, Malaise M, de Seny D. Chondrocyte dedifferentiation and osteoarthritis (OA). Biochem Pharmacol 2019;165:49-65. https://doi.org/10.1016/j.bcp.2019.02.036
6. Wang J, Liu S, Shi J, Li J, Wang S, Liu H, Zhao S, Duan K, Pan X, Yi Z. The Role of miRNA in the Diagnosis, Prognosis, and Treatment of Osteosarcoma. Cancer Biother Radiopharm 2019;34:605-613. https://doi.org/10.1089/cbr.2019.2939
7. Le LT, Swingler TE, Clark IM. Review: the role of microRNAs in osteoarthritis and chondrogenesis. Arthritis Rheum 2013;65:1963-1974. https://doi.org/10.1002/art.37990
8. Jones SW, Watkins G, Le Good N, Roberts S, Murphy CL, Brockbank SM, Needham MR, ET AL. The identification of differentially expressed microRNA in osteoarthritic tissue that modulate the production of TNF-alpha and MMP13. Osteoarthritis Cartilage 2009;17:464-472. https://doi.org/10.1016/j.joca.2008.09.012
9. Zhang W, Hu C, Zhang C, Luo C, Zhong B, Yu X. MiRNA-132 regulates the development of osteoarthritis in correlation with the modulation of PTEN/PI3K/AKT signaling. BMC Geriatr 2021;21:175. https://doi.org/10.1186/s12877-021-02046-8
10. Wang H, Wang W, Wang J, Zhang L, Luo Y, Tang X. MicroRNA-15a/beta1,4-GalT-I axis contributes to cartilage degeneration via NF-kappaB signaling in osteoarthritis. Clinics (Sao Paulo) 2023;78:100254. https://doi.org/10.1016/j.clinsp.2023.100254
11. Sun Y, Su S, Li M, Deng A. Inhibition of miR-182-5p Targets FGF9 to Alleviate Osteoarthritis. Anal Cell Pathol (Amst) 2023;2023:5911546. https://doi.org/10.1155/2023/5911546
12. Zhou J, Su M, Zhang H, Wang J, Chen Y. miR-539-3P inhibits proliferation and invasion of gastric cancer cells by targeting CTBP1. Int J Clin Exp Pathol 2019;12:1618-1625.
13. Wang Z, Hu T, Jin C, Yu J, Zhu D, Liu J. The anti-tumor effect of miR-539-3p on colon cancer via regulating cell viability, motility, and nude mouse tumorigenicity with CDK14 inhibition. J Gastrointest Oncol 2020;11:899-910. https://doi.org/10.21037/jgo-20-387
14. Gong YB, Fan XH. MiR-539-3p promotes the progression of epithelial ovarian cancer by targeting SPARCL1. Eur Rev Med Pharmacol Sci 2019;23:2366-2373. https://doi.org/10.26355/eurrev_201903_17381
15. Yang Z, Hao J, Hu ZM. MicroRNA expression profiles in human adipose-derived stem cells during chondrogenic differentiation. Int J Mol Med 2015;35:579-586. https://doi.org/10.3892/ijmm.2014.2051
16. Qin F, Wang F, Wang XP, Chen J, Zeng FH, Sun CL, Mao JP, Li CL. MiR-539-3p inhibited chondrogenic differentiation in human adipose stem cells by targeting Sox9. J Orthop Surg Res 2022;17:168. https://doi.org/10.1186/s13018-022-03053-0
17. Kim IS, Otto F, Zabel B, Mundlos S. Regulation of chondrocyte differentiation by Cbfa1. Mech Dev 1999;80:159-170. https://doi.org/10.1016/S0925-4773(98)00210-X
18. Zheng Q, Zhou G, Morello R, Chen Y, Garcia-Rojas X, Lee B. Type X collagen gene regulation by Runx2 contributes directly to its hypertrophic chondrocyte-specific expression in vivo. J Cell Biol 2003;162:833-842. https://doi.org/10.1083/jcb.200211089

19. Hirata M, Kugimiya F, Fukai A, Saito T, Yano F, Ikeda T, Mabuchi A, ET AL. C/EBPbeta and RUNX2 cooperate to degrade cartilage with MMP-13 as the target and HIF-2alpha as the inducer in chondrocytes. Hum Mol Genet 2012;21:1111-1123. https://doi.org/10.1093/hmg/ddr540
20. Kamekura S, Kawasaki Y, Hoshi K, Shimoaka T, Chikuda H, Maruyama Z, Komori T, ET AL. Contribution of runt-related transcription factor 2 to the pathogenesis of osteoarthritis in mice after induction of knee joint instability. Arthritis Rheum 2006;54:2462-2470. https://doi.org/10.1002/art.22041
21. Wang Y, Zheng X, Luo D, Xu W, Zhou X. MiR-99a alleviates apoptosis and extracellular matrix degradation in experimentally induced spine osteoarthritis by targeting FZD8. BMC Musculoskelet Disord 2022;23:872. https://doi.org/10.1186/s12891-022-05822-8
22. Pritzker KP, Gay S, Jimenez SA, Ostergaard K, Pelletier JP, Revell PA, Salter D, van den Berg WB. Osteoarthritis cartilage histopathology: grading and staging. Osteoarthritis Cartilage 2006;14:13-29. https://doi.org/10.1016/j.joca.2005.07.014
23. Zhang Z, Zhao T, Xu H, Wu X. Circ_0008365 Suppresses Apoptosis, Inflammation and Extracellular Matrix Degradation of IL-1beta-treated Chondrocytes in Osteoarthritis by Regulating miR-324-5p/BMPR2/NF-kappaB Signaling Axis. Immunol Invest 2022;51:1598-1611. https://doi.org/10.1080/08820139.2021.2001496
24. Miyaki S, Asahara H. Macro view of microRNA function in osteoarthritis. Nat Rev Rheumatol 2012;8:543-552. https://doi.org/10.1038/nrrheum.2012.128
25. Liu Y, Qian K, Li C, Ma Y, Chen X. Roles of microRNA-539 and osteopontin in rheumatoid arthritis. Exp Ther Med 2018;15:2681-2687. https://doi.org/10.3892/etm.2017.5665
26. Peng Y, Jiang H, Zuo HD. Factors affecting osteogenesis and chondrogenic differentiation of mesenchymal stem cells in osteoarthritis. World J Stem Cells 2023;15:548-560. https://doi.org/10.4252/wjsc.v15.i6.548
27. Hu X, Miao H. MiR-539-5p inhibits the inflammatory injury in septic H9c2 cells by regulating IRAK3. Mol Biol Rep 2022;49:121-130. https://doi.org/10.1007/s11033-021-06849-1
28. Meng L, Cao H, Wan C, Jiang L. MiR-539-5p alleviates sepsis-induced acute lung injury by targeting ROCK1. Folia Histochem Cytobiol 2019;57:168-178. https://doi.org/10.5603/FHC.a2019.0019
29. Martel-Pelletier J, Boileau C, Pelletier JP, Roughley PJ. Cartilage in normal and osteoarthritis conditions. Best Pract Res Clin Rheumatol 2008;22:351-384. https://doi.org/10.1016/j.berh.2008.02.001
30 Liacini A, Sylvester J, Li WQ, Zafarullah M. Mithramycin downregulates proinflammatory cytokine-induced matrix metalloproteinase gene expression in articular chondrocytes. Arthritis Res Ther 2005;7:R777-R783. https://doi.org/10.1186/ar1735
31. Akhtar N, Rasheed Z, Ramamurthy S, Anbazhagan AN, Voss FR, Haqqi TM. MicroRNA-27b regulates the expression of matrix metalloproteinase 13 in human osteoarthritis chondrocytes. Arthritis Rheum 2010;62:1361-1371. https://doi.org/10.1002/art.27329
32. Li Z, Cheng J, Liu J. Baicalin Protects Human OA Chondrocytes Against IL-1beta-Induced Apoptosis and ECM Degradation by Activating Autophagy via MiR-766-3p/AIFM1 Axis. Drug Des Devel Ther 2020;14:2645-2655. https://doi.org/10.2147/DDDT.S255823
33. Lopponen T, Korkko J, Lundan T, Seppanen U, Ignatius J, Kaariainen H. Childhood-onset osteoarthritis, tall stature, and sensorineural hearing loss associated with Arg75-Cys mutation in procollagen type II gene (COL2A1). Arthritis Rheum 2004;51:925-932. https://doi.org/10.1002/art.20817
34. Shukla GC, Singh J, Barik S. MicroRNAs: Processing, Maturation, Target Recognition and Regulatory Functions. Mol Cell Pharmacol 2011;3:83-92.
35. Takeda S, Bonnamy JP, Owen MJ, Ducy P, Karsenty G. Continuous expression of Cbfa1 in nonhypertrophic chondrocytes uncovers its ability to induce hypertrophic chondrocyte differentiation and partially rescues Cbfa1-deficient mice. Genes Dev 2001;15:467-481. https://doi.org/10.1101/gad.845101
36. Ueta C, Iwamoto M, Kanatani N, Yoshida C, Liu Y, Enomoto-Iwamoto M, Ohmori T, ET AL. Skeletal malformations caused by overexpression of Cbfa1 or its dominant negative form in chondrocytes. J Cell Biol 2001;153:87-100. https://doi.org/10.1083/jcb.153.1.87
37. Komori T. Molecular Mechanism of Runx2-Dependent Bone Development. Mol Cells 2020;43:168-175. https://doi.org/10.14348/molcells.2019.0244

38. Cao J, Han X, Qi X, Jin X, Li X. miR-204-5p inhibits the occurrence and development of osteoarthritis by targeting Runx2. Int J Mol Med 2018;42:2560-2568. https://doi.org/10.3892/ijmm.2018.3811
39. Li C, Li W, Pu G, Wu J, Qin F. Exosomes derived from miR-338-3p-modified adipose stem cells inhibited inflammation injury of chondrocytes via targeting RUNX2 in osteoarthritis. J Orthop Surg Res 2022;17:567. https://doi.org/10.1186/s13018-022-03437-2